



A plastic scintillator-based activity monitor for tritiated water in the GBq/ℓ range



Zoltán Köllő

Karlsruhe Institute of Technology, Institute of Technical Physics, Tritium Laboratory, Hermann-von-Helmholtz-Platz 1, 76344 Eggenstein-Leopoldshafen, Germany

ARTICLE INFO

Article history:

Received 5 February 2015

Received in revised form

25 June 2015

Accepted 25 June 2015

Available online 10 July 2015

Keywords:

Tritium

Tritiated water

Scintillator

Photomultiplier

Scintillator damage

ABSTRACT

The measurement of tritium activity in water in the GBq/ℓ range is an important topic in fusion and other areas. In this work a scintillator detector based on the BC-408 plastic scintillator was built up and tested in the mentioned range. The structure of the detector was simplified to ease maintenance. Memory effect and scintillator damage were investigated by means of experiment and simulation. The results are analyzed in view of further detector development, and conclusions are drawn concerning the scintillator material.

© 2015 Elsevier B.V. All rights reserved.

1. Introduction

The monitoring of tritium levels in water is important not only for environmental protection purposes, but also for the safe operation of tritium handling facilities. In tritium laboratories, like the Tritium Laboratory Karlsruhe (TLK, [1]), substantial amounts of tritiated water are produced during the detritiation of the glove box or the laboratory atmosphere. This water has to be treated in a water detritiation system (WDS, [2,3]), to recover tritium and minimize releases to the environment. Such a facility is foreseen also for the fusion reactors JET [4] and ITER [5].

Since tritiated water (HTO) is toxic, but behaves chemically as normal water, direct handling is better to be avoided; therefore an inline measurement method is preferable [6]. To monitor the processes in the WDS, it is advantageous to have a near-to-realtime activity measurement. Taking the time constants of such processes (on the order of some hours [3]) into account, the activity concentration of the water should be measured at least every 10 min, in order to follow the process. The detection limit of the detector (considering the concentration range in a WDS, [3]) should be on the order of MBq/ℓ, with measurement range up to the GBq/ℓ region.

The standard method to measure tritium in water is liquid scintillation counting (LSC) [7]. However, this method is offline, requires direct handling of tritiated water and produces

radioactive, organic waste, which makes it undesirable for purposes of process monitoring. A detector with solid scintillator, however, has none of these disadvantages and can be made an online monitor. Such detectors have been fabricated in the past (see Section 2.2), but these were constructed to measure HTO only in the kBq/ℓ range. Therefore the goal of this work was to build and test a detector for the GBq/ℓ range.

2. Measurement of tritium activity in water

2.1. Challenges of tritium measurement

Tritium is a weak beta emitter with 18.6 keV maximal beta electron energy. This means that the average penetration depth of tritium beta electrons in liquid and solid materials is in the micrometer range [8]. Thus, the size of the surface of a solid tritium-in-water detector is the main factor in detection efficiency. Additionally, the low penetration depth makes the detection of tritium in general more challenging than the detection of other beta emitters with higher energy.

Semiconductor devices for radiation measurement usually have to be cooled below the freezing point of water to have low and stable noise; therefore these are not ideal for tritium detection in water. They can be used for indirect detection with the BIXS technique [9], but such detectors require thin beryllium windows (some hundred micrometer in thickness [9]) as a primary containment. This poses a hazard for WDS systems with overpressure (WDS facilities can work

E-mail address: kolloz42@gmail.com

with up to some bar overpressure [3]). The detection limit of such a detector for water is reported by Matsuyama et al. to be 3 MBq/ℓ, which is adequate for a WDS. A sensitivity of 5.5×10^{-9} cps/(Bq/ℓ) was obtained, which is several orders of magnitude lower than those of scintillation counters (see Section 2.2). However, the BIXS technique is still considered as a promising method to measure tritiated water in the GBq/ℓ to TBq/ℓ range [10].

Solid scintillator detectors are a better solution, because the scintillator can be placed into the water for direct detection of the tritium beta electrons. The scintillation light can be detected outside the sample chamber, meaning a safe separation of most of the detector components from the tritiated water by means of a thick glass window. Because of possible contamination of the components, an HTO-detector has to be maintained in a fume hood or a glove box. For easier maintenance the detector should have a simple structure (see also Section 3.1). Since radicals are produced in HTO by the radiation [11], such water can damage materials; therefore scintillator damage is a possibility, which needs to be investigated.

2.2. Previous works

Several authors built detectors for tritium in water based on scintillators (see Refs. [12–16]). In these studies various organic scintillators in various forms were used, and the scintillation light was measured with PMTs in coincidence mode.

The detection limits of the various detectors were all in the kBq/ℓ range, but the detection efficiencies scatter over a wide range of four orders of magnitude (3.85×10^{-4} to 3.2 cps/(Bq/ℓ)). For a better comparison of the various detectors it is useful to calculate the detection efficiency per unit scintillator surface:

$$\epsilon = \frac{CR}{c_A \cdot F_{sci}} \quad (1)$$

where CR is the count rate of the detector, c_A is the tritium concentration of the water, and F_{sci} is the surface area of the scintillator.

The specific efficiencies calculated from the values reported in the mentioned works are all in the range of 10^{-6} – 10^{-5} cps/(Bq/ℓ cm²). Considerable memory effect and scintillator damage was not reported, probably due to the low concentration range of kBq/ℓ. However, Osborne [14] reported deterioration of the scintillator in hydrochloric acid, which caused a sensitivity decrease after 130 days.

2.3. Scope of this work

In this study a test setup to measure tritium in water was built and investigated. No flow chamber was built because the goal was the testing of the concept for higher concentrations. The detector was simplified as much as possible to ease maintenance (see Section 3.1). A plastic scintillator was used because it can be easily formed and was successfully used for low concentration in previous studies [15]. For light detection, a PMT was used because the average number of scintillator photons per decay electron was expected to be low. Indeed, for a 5.7 keV electron (average beta energy of tritium), the average number of photons from the scintillator used in the study (see next section) is around 32 (calculated by integrating the Birks equation [19], using stopping power data from the ESTAR database [8]).

The main goals of this study were

- build and test a detector with simple construction
- analysis of the detection process of the detector with experiments and simulation
- measurements in the concentration range up to about 30 GBq/ℓ

- measurement of sensitivity and detection limit, and comparison of the results with those obtained by the BIXS method [9,10].
- investigation of memory effect and/or short term scintillation damage and
- general conclusions about scintillators used in tritiated water detectors for high concentration

3. Experimental setup

3.1. Overview

The cross-section of the setup is depicted in Fig. 1. The simplification of the detector structure meant that only one PMT was used. For easier maintenance the direct light coupling from the sample chamber to the PMT was omitted. It would have involved the application of optical grease and additional elements, and this would complicate maintenance. The latter is already complicated if good contamination control with tritiated water is to be assured.

The outer shell of the setup was cooled to 15 °C to minimize background drift due to ambient temperature changes, but not so cool as to allow condensation. The cooling was ensured by means of a commercially available water cooling unit [20], and a plastic tube carrying the cooling water, wrapped around the whole setup. The stability of the water temperature was at least 0.1 °C. The components are detailed in the following sections.

3.2. Scintillator

As a plastic scintillator, the BC-408 [17] material (produced by Saint-Gobain Crystals) was used. This material has a light yield of 64% compared to that of anthracene, its emission maximum is at 425 nm. The circular scintillator disk with a diameter of 29 mm has been cut out from a 0.5 mm thick polished plate. The disk was put onto a holder made of a 1 mm thick stainless steel wire (see Fig. 2) to keep it away from the bottom of the sample chamber, so that the whole surface of the scintillator is in contact with the tritiated water.

3.3. Sample chamber

The sample chamber consists of the metal outer shell, a glass cup to hold the tritiated water and the scintillator, and a quartz window towards the PMT for the scintillation light. The glass cup was 51 mm tall, with an inner diameter of 30 mm and a wall thickness of 2 mm (Fig. 2). A polished aluminum cylinder was used to cover the glass cup on the top and the side for better light reflection (this part was omitted in Fig. 1 for clarity).

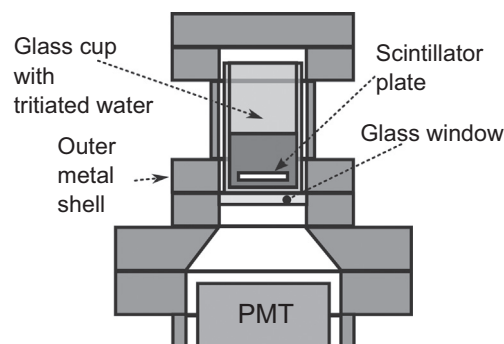


Fig. 1. Cross-section-view of the main part of the setup. The aluminum cup which surrounds the glass cup (but leaves the bottom open) is not shown for clarity (it is presented in Fig. 2). The space between the PMT and the glass window is filled with air. The figure is to scale.

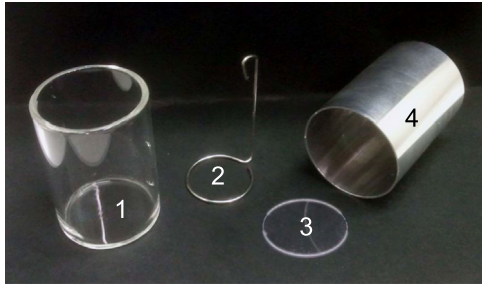


Fig. 2. Inner parts of the sample chamber. (1) Glass cup, (2) scintillator holder, (3) scintillator, (4) aluminum cup.

3.4. Signal readout

As a light detector, a Photonis XP-2262 PMT was used, which has a bialkali photocathode with a quantum efficiency of 26.5% at the emission maximum of the scintillator. The supply voltage was 1850 V. The signal of the PMT was processed by means of Ortec instruments: a type 113 scintillation amplifier, a 575A main amplifier and an Easy-MCA-8k multichannel analyzer. The signal pulse threshold was set to measure also single photoelectron events. The background count rate of the PMT (cooled to 15 °C) was around 300 cps.

4. Simulation of detector response

It was important to analyze the theoretically possible spectrum for different light yields, since scintillator damage is a possibility. Damage of the scintillator material decreases its light yield [19].

4.1. Description of the simulation

The detector response was simulated by means of the GEANT4 simulation package [21]. The standard electromagnetic physics list was used, including bremsstrahlung and ionization for electrons, Compton scattering and ionization for gamma photons, and scintillation processes for both. The simulation was written utilizing the GAMOS framework [22]. The necessary parameters were taken from the ESTAR database [18], the data sheets of the detector components, and from Refs. [23–27]. The complex refraction index of stainless steel was not available from any database. Therefore, it was substituted with that of iron, which is the main constituent of stainless steel. The obtained data was post-processed with a custom-written C program to simulate the Birks quench and to calculate the results for several scintillation yields.

The geometry in the simulation follows the geometry in Fig. 1. The parts are built up using cylinders and cones, all surfaces have been defined to be smooth, because the metal surfaces in the experimental setup are polished and the glass surfaces are also smooth.

The program simulates the detection process from the decay electrons until the scintillation photons are absorbed in the photocathode or elsewhere in the setup. The number of photoelectrons detected in the PMT is counted for each decay event, taking into account the wavelength-dependent quantum efficiency of the PMT. The result of the simulation is the photoelectron-number spectrum (or electron number spectrum) “measured” with the simulated PMT.

4.2. Results for different light yields

The simulation has been executed for a Birks parameter of $kB = 9.21 \cdot 10^{-3} \text{ g}/(\text{MeV cm}^2)$ [24]. The light yield ratio $Y = S_{sim}/S_{orig}$ (where S_{sim} is the light yield in the simulation and $S_{orig} = 9600 \text{ photons/MeV}$

that of BC-408) was 100, 50 and 10%. The results are shown in Fig. 3. Clearly, the light yield has a significant impact on the spectrum. With the original light yield the maximum observable electron number in an event is 14, but with 10% only 4, while the sensitivity is $1.8 \times 10^{-8} \text{ cps}/(\text{Bq}/\ell \text{ cm}^2)$ and $4.1 \times 10^{-9} \text{ cps}/(\text{Bq}/\ell \text{ cm}^2)$, respectively. The theoretical maximal sensitivity is about two orders of magnitude lower than those of previous scintillator detectors. The reason is that only 25.5% of photons arrive to the photocathode (as calculated from the simulation results) due to light absorption in the setup, which is the consequence of the light coupling being omitted. However, this sensitivity is much higher than that of the BIXS method (Section 2.2 and [9]), and could be adequate for HTO in the GBq/ ℓ range. The simulation does not give a detection limit, because it depends also on the background stability of the PMT. This is discussed in Section 5.2.

5. Measurements and data analysis

5.1. Measuring the spectrum of tritiated water

The measurement was performed as follows: the sample chamber was filled with 3 ml of tritiated water with a concentration of $5.86 \pm 0.07 \text{ GBq}/\ell$. The sample chamber was closed and the PMT high voltage was switched on. The pulse height spectrum of the PMT was measured for several days, because the photocathode was exposed to ambient light and this increased the background substantially. After the signal has stabilized, 10-min measurements of the spectrum was performed 100 times in succession. The spectra were then added, corrected for deadtime and normalized with the measurement time. It was assumed, that the single electron peak (SEP) can be described with a Gaussian curve, and the multiple electron peaks are simply the result of single electron events happening at the same time. Based on these assumptions the following fitting function has been fitted to the measured spectrum:

$$C(CH) = \sum_{n=1}^M \frac{C_n}{\sqrt{2\pi n} \cdot \sigma_{SEP}} \cdot \exp\left(-\frac{1}{2} \left(\frac{CH - n \cdot PP_{SEP}}{\sqrt{n} \cdot \sigma_{SEP}}\right)^2\right). \quad (2)$$

This is a sum of Gaussian curves, where $C(CH)$ is the number of counts in the CH th channel of the ADC, n means the number of photoelectrons in an event, C_n is the number of events with n photoelectrons, M is the maximum number of photoelectrons in an event, PP_n is the center of the n th Gaussian (the peak position), and σ_{SEP} is the standard deviation of the single electron peak. Only the spectrum part from channel 160 was used for the fitting, since below this channel the spectrum deviated from the sum of Gaussians because of unavoidable noise pulses. The resulting

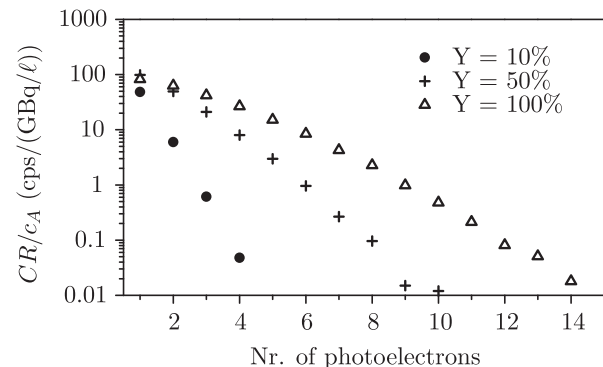


Fig. 3. Simulated spectra with various yield factors (Y). $Y = S_{sim}/S_{orig}$, where S_{sim} and S_{orig} are the light yields of the scintillator in the simulation and that of BC-408, given by the manufacturer, respectively.

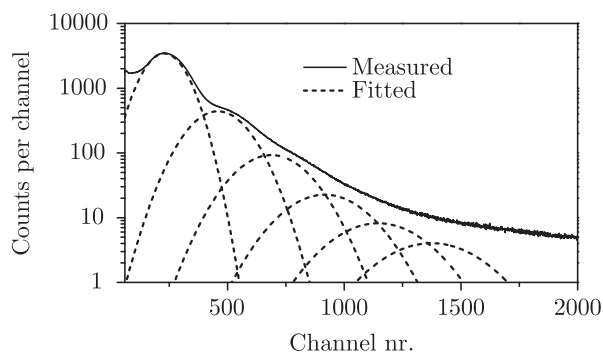


Fig. 4. The measured HTO spectrum and the first six fitted Gaussian curves. The counts in the channels are calculated for 10 min livetime. Above channel 1600 the HTO spectrum did not differ significantly from the background. As a consequence, from the 7th Gaussian, the areas under the Gaussian curves for background and HTO were the same within error, therefore these are not shown.

Gaussian curves, together with the measured spectrum are displayed in Fig. 4.

The correlation coefficient between the fitted curve and the measured one was 0.9998, meaning an excellent fit. The same measurement and fitting procedure was performed for the background of the setup with distilled water. It was found that the areas of the Gaussian curves above six-electron events (count of events with seven or more photoelectrons) match the background within error, meaning maximum six-electron-events were detectable on the HTO spectrum. The background counts were subtracted from the HTO counts and the sensitivity of the detector was calculated to be 1.39×10^{-8} cps/(Bq/ℓ·cm²). This is much lower than the one obtained from the simulation with the scintillator light yield given by the manufacturer. The reason is most probably a damage of the scintillator, which can alter the scintillation yield. The scintillator damage can be caused by the radicals in the water, as well as the radiation.

A chi-square optimization was performed with the simulation data, by changing the scintillation yield and the Birks parameter (which can also be different due to scintillator damage) to fit the simulated electron number spectrum to the experimental one. The optimized parameters, yielding the lowest reduced chi-square value of 275.3, were $kB=0.0$ and $Y = 17.5 \pm 0.5\%$. The comparison of the experimental and the optimized simulated spectrum is displayed in Fig. 5.

The reduced chi-square value being well over 1.0 indicates that the fit is far from being perfect. However, if the reduced chi-square is calculated only above the single electron peak, the value reduces to 31.4, meaning that the simulated single electron peak deviates the most from the experimentally measured one. The reason for this is probably the afterpulses of the PMT, which are mostly single electron events, indistinguishable from real signals.

5.2. Measurements with different tritium concentrations

The setup was modified for further experiments, as it is described in Appendix A. The main structure however, remained the same, except that the PMT was protected from ambient light by means of a sliding valve during sample change.

The background of the detector was measured continuously in a one week period, with 5 ml distilled water in the sample chamber. The measurement time of the individual data points during the presented measurements was always 10 min. The background value was between 894 and 904 cps, the slight drifts attributed to minor changes in detector temperature.

The setup was then calibrated by means of five tritiated water samples with concentrations from 3.11 to 27.45 GBq/ℓ. In-between the HTO measurements the tritiated water was taken out from the

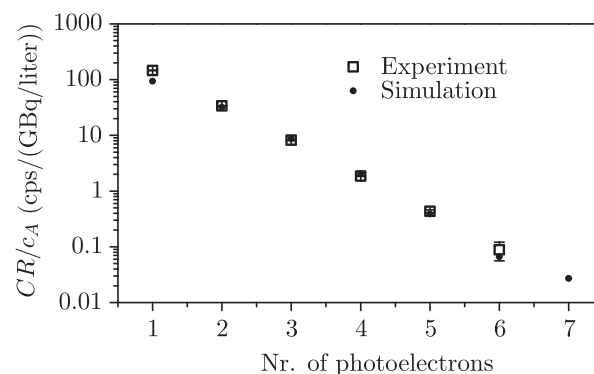


Fig. 5. Comparison of the optimized simulated spectrum with the experiment. The main parameters of the simulation: $kB=0.0$ g/(MeV cm²), $S_{sim} = 1680$ photons/MeV.

sample chamber, the glass cup and the scintillator were rinsed with distilled water and distilled water filled in. The water amount was always 5 ml. The threshold of the counting electronics was set in the valley between the SEP and the noise, and the total count rate of the detector was measured for each sample. A linear detector response was obtained: the correlation coefficient between the concentration and the count rate was 0.9996.

The background count rate increased during the measurement series, which implies a memory effect. The background, 24 h after the last HTO measurement, was more than 50 cps higher than the background in the beginning. It took a month for the count rate to decrease to 904 cps, just in the range of the background in the beginning.

After the measurements the scintillator was taken out from the setup, and rinsed with distilled water 3 times. Then it was dissolved in 15 ml InstaGel scintillator cocktail, and measured in the same LSC machine, as the one used for the water samples.¹ The scintillator plate contained 12 Bq tritium, which evidences a retention of tritium in the scintillator. The tritium retention is most probably responsible for the memory effect. The detection limit is high due to the memory effect: if one takes the highest measured background into consideration, the signal shall be higher than that value. If the detection limit is calculated according to Ref. [28], using the highest measured background and its standard deviation, its value is 29 MBq/ℓ, which is high compared to the target value mentioned in Section 1.

Besides the memory effect, the signal of the detector showed a delay after exposing the PMT to the samples (i.e. opening the sliding valve; see Fig. 6). The analysis of the signals is described in Appendix B. It took about 1.5 h for the signal to reach its final value during a HTO measurement and about 2–2.5 h to approximately stabilize in the case of background measurements. The background also drifted after the measurement of the two highest HTO concentrations. As detailed in Appendix B, this behavior can be attributed to the adsorption/desorption of tritiated molecules on the surface of the scintillator. Such a delay limits the usage of such detectors to monitor processes which have time constants longer than 2.5 h.

6. Conclusions and outlook

A plastic scintillator-based detector was constructed and tested for tritiated water in the GBq/ℓ concentration range. The actual measured sensitivity of the detector is lower than that in the

¹ The LSC machine was tested by means of samples with and without dissolved plastic scintillator, the resulting correction is included in the result.

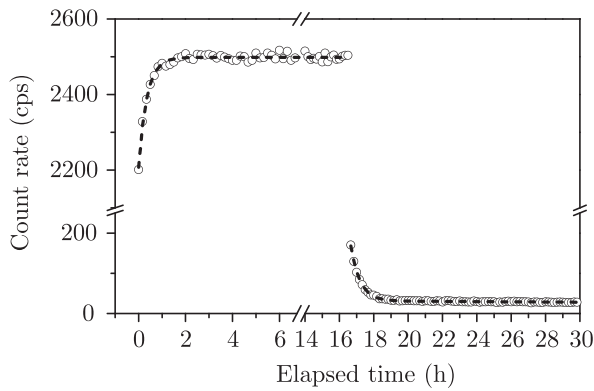


Fig. 6. Response of the detector to tritiated water and distilled water afterwards. Only the DEP count rate is displayed (see Appendix B). Tritiated water concentration: 27.45 ± 0.31 GBq/ℓ. The elapsed time is measured from the beginning of the first measurement after opening the sliding valve. The dashed lines show the fit result using Eqs. (B.1), (B.3) and (B.4) (see Appendix B).

simulation, due to (most probably) the damage of the scintillator surface by tritiated water. A considerable memory effect is also observable, which was not an issue for concentrations in the kBq/ℓ range. This increases the detection limit significantly above the desired 1 MBq/ℓ. Besides that, the signal of the detector does not react instantaneously to the change in the sample concentration, but shows 1.5–2.5 h delay in reaching the stable value. The last two effects are attributed to the (time-dependent) adsorption/desorption of tritiated molecules onto/from the scintillator. Such effects are not favorable for a WDS which has time constants of less than some hours.

The issues above imply, that a plastic scintillator material is not the most adequate to be used in a detector for the GBq/ℓ concentration range. Another, more resistant material, e.g. a YAP scintillator [29] however, may be satisfactory, though confirmation awaits future measurements.

Acknowledgments

The author wishes to thank Guido Drexlin, professor of physics at KIT, and Beate Bornschein, leader of TLK for helpful discussions during this work. The help and useful advices of Robert Michling and Stefan Welte from TLK and those of Joachim Wolf from the Nuclear Physics Institute at KIT are greatly appreciated. Contributions from Sebastian Schler in the beginning phase of this study were also valuable. This research was funded by the Fusion Program of KIT.

Appendix A. Modifications on the setup

The PMT in the first experiments had to be switched off if the sample chamber was to be opened, and it took two days until the PMT signal was stabilized. This makes it impossible to follow the short-term reaction of the detector to sample change. Therefore, the setup was modified as follows:

- The sample chamber was redesigned, so that the glass cup is fixed at the top of the chamber. This makes the quartz window unnecessary (which was holding the glass cup before).
- The glass cup inner diameter and the scintillator diameter was enlarged to 40 and 39 mm, respectively.
- In place of the window, a sliding valve was built in, which provides leak-tight protection of the PMT.

- A new PMT, type 9813B from ET-Enterprises, has been built in. It has a larger gain ($7 \cdot 10^7$) than the previously used one, but other characteristics are similar (bialkali cathode, quantum efficiency, etc.).

Appendix B. Analysis of the time dependence of the detector signal

As it is mentioned in Section 5.2, the measured count rate did not change abruptly after changing the HTO concentration and opening the sliding valve, but increased/decreased gradually in the case of HTO/background measurements. To investigate this phenomenon, the double-electron peak (DEP²) was used. The reason for this is that the DEP is still significant in the spectrum, but minor temperature changes do not affect it (unlike the SEP). The DEP count rates were determined for every 10-min measurement by fitting (2) to each measured spectrum. The count rates of a typical HTO and a following background measurement are presented in Fig. 6.

As a theoretical description of the above, the following model is proposed: the count rate of the detector is the sum of three components, the background (BG), the count rate proportional to the concentration in the water (concentration: c_A), and the count rate due to tritiated molecules on the surface of the scintillator (number of molecules on the surface: N_{sur}):

$$CR = BG + K_1 \cdot c_A + K_2 \cdot N_{sur}. \quad (B.1)$$

The number of tritiated molecules on the surface is supposed to change according to the following equation:

$$\frac{dN_{sur}}{dt} = c_A H - \frac{N_{sur}}{\tau} \quad (B.2)$$

where H is a constant and τ is the mean time one molecule spends on the surface. The first term says that the speed of adsorption is proportional to the tritium concentration in the water and the second term expresses that the rate of desorption is proportional to the number of molecules on the surface. This equation has basically the same form as the Lagergren equation [30], which is the simplest equation describing adsorption kinetics.

Assuming a clean scintillator placed into HTO with concentration c_A , the solution to Eq. (B.2) is

$$N_{sur} = c_A H \tau (1 - \exp(-t/\tau)). \quad (B.3)$$

By placing this function into Eq. (B.1) one can fit the parameters (H and τ) to the experimental data, as shown in Fig. 6. This fit was done for all HTO measurement data series, yielding fitted parameter values with errors under 10%. The obtained values of τ were the same within experimental error, giving $\tau = 21.0$ min as average.

According to Eq. (B.3), the coefficient of the exponential should be directly proportional to c_A . The correlation coefficient between the experimentally obtained values is 0.9668, meaning a fair correlation. These results imply that this simple model of adsorption approximately describes the observed process.

In case the scintillator is in distilled water, and there are N_0 tritiated molecules on the surface of it in the beginning, the solution to Eq. (B.2) is

$$N_{sur} = N_0 \exp(-t/\tau') \quad (B.4)$$

where τ' is a time constant as in (B.2), but its value can be different in the case of desorption in distilled water, because some of the tritiated molecules can diffuse into the scintillator material slightly while the scintillator is in HTO. The effect of this is approximated

² Events, where two photoelectrons are detected.

here by allowing a longer desorption time. Eq. (B.1) with Eq. (B.4) in place of N_{sur} was fitted to the data obtained from the background measurements. A second exponential was added to it with independent parameters, which was necessary to describe the slow drift of the background 4–5 h after the start of the measurement. This drift can mean molecules which were strongly bonded to the scintillator, thus having an even longer desorption time. The obtained values for τ' were the same within error, the average value was 30 min, with errors less than 5%. The time constants of the slow drift were on the order of 300 min, but with errors up to 40%. This can mean that the second exponential as a model of the drift is not accurate.

Osborne [14] observed a similar behavior in a flow cell detector, but the time constants were much shorter, under 10 min. This can be attributed to the different scintillator material and/or the flow of water, which can alter the adsorption/desorption process.

In conclusion, the delayed response of the detector can be approximately described by assuming adsorption/desorption of tritiated molecules, but the details of the diffusion into and out of the scintillator, the bonding of molecules and the effect of water flow needs to be investigated further.

References

- [1] B. Bornschein, *Fusion Science and Technology* 60 (2011) 1088.
- [2] I. Christescu, et al., *Fusion Engineering and Design* 82 (2007) 2126.
- [3] R. Michling, et al., *Fusion Engineering and Design* 84 (2009) 338.
- [4] A.N. Perevezentsev, et al., *Fusion Engineering and Design* 61–62 (2002) 585.
- [5] M. Glugla, et al., *Fusion Engineering and Design* 82 (2007) 472.
- [6] B. Bornschein, et al., *Fusion Engineering and Design* 88 (2013) 466.
- [7] D.L. Horrocks, *Applications of Liquid Scintillation Counting*, Academic Press, Inc., New York and London, 1974.
- [8] ESTAR database (<http://physics.nist.gov/PhysRefData/Star/Text/ESTAR.html>), 2015 (accessed 23.01.2015).
- [9] M. Matsuyama, Y. Torikai, K. Watanabe, *Fusion Science and Technology* 48 (2005) 324.
- [10] M. Matsuyama, *Fusion Engineering and Design* 83 (2008) 1438. <http://dx.doi.org/10.1016/j.fusengdes.2008.05.023>.
- [11] T. Stolz, et al., *Fusion Engineering and Design* 69 (2003) 57.
- [12] M. Muramatsu, A. Koyano, N. Tokunaga, *Nuclear Instruments and Methods in Physics Research* 54 (1967) 325.
- [13] A.A. Moghissi, et al., *Nuclear Instruments and Methods in Physics Research* 68 (1969) 159.
- [14] R.V. Osborne, *Nuclear Instruments and Methods in Physics Research* 77 (1969) 170.
- [15] A.N. Singh, M. Ratnakaran, K.G. Vohra, *Nuclear Instruments and Methods in Physics Research Section A* 236 (1985) 159.
- [16] K.J. Hofstetter, H.T. Wilson, *Fusion Technology* 21 (1992) 446.
- [17] BC-400, BC-404, BC-408, BC-412, BC-416 Premium Plastic Scintillators. Brochure of the Saint-Gobain Ceramics & Plastics, Inc., 2008.
- [18] Photomultiplier tubes; principles and applications, Photonis, Brive, France, 2002.
- [19] J.B. Birks, *The Theory and Practice of Scintillation Counting*, Pergamon Press, Oxford, 1964.
- [20] "Oasis Three" water chiller, Operating manual, Solid State Cooling Systems, 2011.
- [21] S. Agostinelli, et al., *Nuclear Instruments and Methods in Physics Research Section A* 506 (2003) 250. [http://dx.doi.org/10.1016/S0168-9002\(03\)01368-8](http://dx.doi.org/10.1016/S0168-9002(03)01368-8).
- [22] P. Arce, et al., *Nuclear Instruments and Methods in Physics Research Section A* 735 (2014) 304. <http://dx.doi.org/10.1016/j.nima.2013.09.036>.
- [23] J.C. Ashley, *Radiation Research* 89 (1) (1982) 25 (<http://www.jstor.org/stable/3575681>).
- [24] M. Hirschberg, et al., *IEEE Transactions on Nuclear Science* NS-39 (4) (1992) 511.
- [25] E.D. Palik, *Handbook of Optical Constants of Solids II*, Academic Press, Inc., Boston, 1991.
- [26] A.D. Rakic, *Applied Optics* 34 (1995) 4755. <http://dx.doi.org/10.1364/AO.34.004755>.
- [27] I.H. Malitson, *Journal of the Optical Society of America* 55 (1965) 1205. <http://dx.doi.org/10.1364/JOSA.55.001205>.
- [28] G.F. Knoll, *Radiation Detection and Measurement*, 4th Edition, John Wiley and Sons, Inc., Hoboken, New Jersey, 2010.
- [29] W. Mengesha, et al., *IEEE Transactions on Nuclear Science* NS-45 (3) 456.
- [30] W. Plazinski, W. Rudzinski, A. Plazinska, *Advances in Colloid and Interface Science* 152 (2009) 2.